HIGH-ALTITUDE ROBIN DATA-REDUCTION PROGRAM

By James Luers and Nicholas A. Engler

University of Dayton Research Institute
Dayton, Ohio

SUMMARY

The problem of computing winds and thermodynamic data utilizing the space-time coordinates of a falling sphere becomes complex when the apogeee of the sphere is over 100 km. This paper describes the methodology used in constructing the computer program.

ROBIN/ARCAS SYSTEM

The ROBIN/Arcas system consists of a ROBIN balloon, an Arcas rocket motor, and an AN/FPS-16 tracking radar. The ROBIN sphere is made of $\frac{1}{2}$- mil Mylar inflatable to a diameter of 1 meter containing an internally supported corner reflector. Packaged in a collapsed condition within the nose-cone of a meteorological rocket, it is ejected at the apogee of the rocket and inflated to a super pressure of approximately 10 millibars by vaporization of a liquid such as isopentane. Thus inflated, the ROBIN sphere is tracked from apogee to approximately 30 km altitude by an AN/FPS-16 high-precision tracking radar. The Arcas rocket motor is a 4.5-inch-diameter solid-propellant end-burning rocket capable of carrying the sphere payload to an altitude of 75 km. The FPS-16 tracking radar generates spherical space-time coordinates at digitized increments of 1/10 second. From the space-time coordinates, the meteorological parameters of density, wind, temperature, and pressure are deduced. A discussion of the ROBIN/Arcas system, with some of its advantages and shortcomings, is contained in reference 1.

Early results from the ROBIN/Arcas system whetted man's appetite to extend the passive sphere experiment to altitudes beyond the reach of the Arcas motor. To achieve this dream the Air Force Cambridge Research Laboratories (AFCRL) has experimented with a variety of boosted rocket motors. The most successful of these is the Viper-Dart rocket motor. The Viper-Dart rocket is capable of carrying the ROBIN payload to an apogee of 125 to 140 km. It was anticipated that the extended balloon apogee of 125 km would enable density and perhaps wind measurements to be extended to 100 km.

The data-reduction program designed by Engler (ref. 1) to reduce the data from ROBIN/Arcas flights produced accurate density and wind measurements below an altitude of 70 km. The high-altitude ROBIN/Viper-Dart system, however, produces balloon

velocities and accelerations much larger than the ROBIN/Arcas system. For this reason the smoothing techniques used in the 1965 ROBIN/Arcas program are not optimum for use with the ROBIN/Viper-Dart system. It has been shown by Engler (ref. 2) that the standard ROBIN/Arcas data-reduction program is not satisfactory for use with high-altitude flights. Accepting the recommendations of Mr. Engler, AFCRL has requested the University of Dayton Research Institute (UDRI) to develop a new ROBIN data-reduction program which would result in optimum density and wind measurement for high-altitude rocket launches as well as the standard Arcas rocket. It is the purpose of this paper to discuss the new data-reduction program, to explain the rationale and methodology used to design the program, and to discuss the errors in the winds and thermodynamic data that result from the use of this program.

PROGRAM SPECIFICATIONS

The preliminary specifications for the program consisted of the following items: (a) the program should be optimum for measuring density and wind in the 70 to 100 km region of the atmosphere assuming a balloon apogee of 125 km, (b) the program should also give accurate and reliable density measurements from 30 to 70 km, (c) even though the data-reduction technique need not be optimum for balloon apogees other than 125 km, other balloon apogees between 75 and 140 km should not result in a serious degradation of the meteorological parameters, (d) temperature and pressure accuracies should be commensurate with density accuracy, and (e) the program should accurately determine the altitude of balloon collapse so that density calculations can be terminated.

DENSITY AND WIND MEASUREMENTS

To obtain density, the drag force that the atmosphere exerts upon the sphere must be measured. In the altitude region from 70 to 100 km, the vertical velocities and accelerations are much larger than the horizontal velocities and accelerations. For this reason the drag acceleration is primarily in the vertical direction. Accurate density calculations are thus largely a result of the accuracy to which vertical velocities and accelerations can be measured.

Horizontal winds influence the sphere's trajectory by inducing horizontal excursions in its path in three-dimensional space. These horizontal excursions are used to reconstruct the wind profile. Thus, for measuring wind, the horizontal velocity and acceleration components must be determined accurately.

Since densities depend primarily on vertical measurements and winds depend primarily on horizontal measurements, it is possible to construct a data-reduction scheme which will optimize both wind and density measurements. The data-reduction scheme used to reduce Viper-Dart flights is so designed.

DENSITY

Density is computed by the following equation:

$$\rho = \frac{m(g - \ddot{z} - C_Z)}{\frac{1}{2}C_D A v(\dot{z} - W_Z) + V_B g} \tag{1}$$

The symbols are defined in the appendix. The computed density error is a result of the errors present in the parameters on the right side of equation (1). A negligible contribution to the error in density is made by V_B, C_Z, g, m, and A. The remaining variables which make a significant contribution to density error are C_D, $\dot{z}$, $\ddot{z}$, W_Z, and v.

DENSITY ERROR EQUATIONS

For the purpose of deriving an error equation for density, the density equation (eq. (1)) can be simplified to

$$\rho = \frac{m(g - \ddot{z})}{\frac{1}{2}C_D A(\dot{z} - W_Z)^2} \tag{2}$$

where v has been set equal to $(\dot{z} - W_Z)$ and both buoyancy and Coriolis force have been neglected.

Considering the error in density to be a function of the errors in C_D, W_Z, $\dot{z}$, and $\ddot{z}$ only and assuming further that the errors in the radar coordinates are independent and normally distributed with mean zero and variance σ, the error equation for the percent error in density is given by

$$\left[\frac{\sigma_\rho}{\rho}\right]^2 = \left[\frac{\sigma_{C_D}}{C_D}\right]^2 + \left[\frac{2\sigma_{W_Z}}{\dot{z} - W_Z}\right]^2 + \left[\frac{\sigma_{\ddot{z}}}{\ddot{z} - g}\right]^2 + \left[\frac{2\sigma_{\dot{z}}}{\dot{z} - W_Z}\right]^2 + \left[\frac{\dot{z}^2(\ddot{z} + \Delta\ddot{z} - g) - (\dot{z} - \Delta\dot{z})^2(\ddot{z} - g)}{(\ddot{z} - g)(\dot{z} + \Delta\dot{z})^2}\right]^2 \tag{3}$$

The object of the computer program as mentioned earlier is to minimize equation (3) in the altitude region from 70 to 100 km. Equation (3) cannot be minimized by minimizing each of the terms on the right-hand side of the equation because the last three terms are

interrelated. The first two terms, however, are independent and thus allow for individual minimization.

ERROR IN DRAG COEFFICIENT

There is no commonly accepted drag table in use today with known accuracy. Of the drag tables being used, disagreements as high as 15% to 20% exist in certain areas (ref. 3). As seen in figure 1, disagreement exists not only between the values of C_D for various drag tables (refs. 4 to 6) but also in the slope of the curves. The drag tables used in previous ROBIN programs designed by UDRI rely primarily on the work of Dr. Helmut Heinrich and others (ref. 5). The accuracy of this table is uncertain especially in areas where interpolation of the drag coefficient is necessary such as from Mach 0.7 to Mach 1.0. In an effort to evaluate the most recent drag table to appear in the literature (ref. 4), UDRI reinvestigated the drag-coefficient values of references 5 and 4. The table which appears as figure 2 is basically the work of reference 5 in the supersonic region and of reference 4 in the subsonic region. The impressive aspect of this drag table is the similar shapes of the C_D curves given as a function of Mach and Reynolds number even though the drag table was the result of two independent researchers using two different techniques for calculating drag. However, even though this drag table shows smooth consistent drag curves, it is impossible to quote specific accuracies of the drag table because of the conflicting results obtained by the other experimenters and because of the interpolated section of the table. The stated accuracies by the experimenters are as follows:

Goin and Lawrence: approximately 2%

Heinrich et al. (supersonic): maximum possible error ranges from ±2.3% to ±27.9%; however, actual errors are usually not the possible maximum

Since the accuracy of the drag table cannot be determined precisely, it is impossible to give an exact RMS error value for the percent error in density when reducing a high-altitude balloon flight. It is, however, possible to determine the error in density that results from the other terms of equation (3). Improvements and verifications of drag results will enable one at some future time to accurately state the true percent error in density.

VERTICAL WIND ERROR

The density error variance resulting from vertical winds is given by the expression $\left[\frac{2\sigma_{W_Z}}{\dot{z} - W_Z}\right]^2$. To a falling sphere, a vertical wind looks identical to a change in density.

As a result, a data-reduction program cannot distinguish density perturbations from vertical-wind oscillations. In order to compute densities, an assumption must be made either concerning vertical winds or concerning density perturbations in the atmosphere.

Assumption A: $W_Z = 0$

Assuming no vertical motions in the atmosphere, equation (1) can be solved by substituting $W_Z = 0$ on the right-hand side of equation (1) and evaluating all other terms by conventional means. Under this assumption, any vertical winds present in the atmosphere will appear as density oscillations. The relationship between vertical winds and density perturbations is exhibited in figure 3 for an escape altitude of 125 km. Care must be used in interpreting figure 3, however, because of the smoothing effect produced in the program. An example will clarify this point. If a sinusoidal vertical wind varying with altitude with amplitude of 5 m/sec is present at 60 km, then this vertical wind would be damped by the smoothing and appear in the printout as something smaller, approximately 2 m/sec amplitude. Since the program attributed the vertical motion to density perturbations, the result of an actual 5 m/sec vertical wind would, using figure 3, appear as a 2.4% density perturbation. To effectively determine what vertical wind could have caused a density perturbation in reduced data in addition to figure 3 one must know the reduction in magnitude of the vertical wind resulting from the smoothing technique applied, i.e., the frequency response of the program's smoothing filter to a sinusoidal vertical-wind oscillation.

Assumption B: $\rho = \rho_0 e^{\alpha z}$

If density is assumed to follow some mean path then perturbations from this path can be attributed to vertical winds. Since density varies exponentially with altitude, a mean exponential path is appropriate. Using this assumption, vertical winds can be computed by the equation

$$W_Z = \frac{\ddot{z}_{th} - \ddot{z}_{emp}}{2K\ddot{z}\rho_0 e^{\alpha z}} \tag{4}$$

A description of the variables in this equation and its application is given in reference 1.

Since, to the best of our knowledge, meteorologists accept density perturbations at least as much as they accept vertical winds, assumption A has been and will be used in this program.

NOISE AND BIAS ERROR TERMS

The remaining terms in the density error equation are given by

$$\left[\frac{2\sigma_{\dot{z}}}{\dot{z} - W_z}\right]^2 + \left[\frac{\sigma_{\ddot{z}}}{\ddot{z} - g}\right]^2 + \left[\frac{\dot{z}^2(\ddot{z} + \Delta\ddot{z} - g) - (\dot{z} - \Delta\dot{z})^2(\ddot{z} - g)}{(\ddot{z} - g)(\dot{z} + \Delta\dot{z})^2}\right]^2 \tag{5}$$

The first two terms of equation (5) are the result of the noise present in the radar coordinates (noise error). The third term is the error in density resulting when the smoothing function does not adequately represent the true path of the sphere. In this case, a bias error will result in density since the smoothing function will not fit the real perturbation in the path.

NOISE ERROR TERMS

The noise errors in vertical velocity ($\sigma_{\dot{z}}$) and acceleration ($\sigma_{\ddot{z}}$) depend upon

The noise present in the radar coordinates (σ_z)
The type of smoothing technique used
The number of data points (N) used in the smoothing process
The time spacing between consecutive data points (Δt)

For an FPS-16 radar, σ_z varies between 10 and 15 meters depending upon slant range and Δt is generally fixed at 0.1 second.

ESTIMATION OF NOISE ERROR

There are two methods of evaluating the noise error terms:

(a) Consider an actual flight of a passive sphere tracked by two identical FPS-16 radars. For an N and a smoothing function, density can be calculated for each of the two radar tracks. By calculating the RMS difference between the densities measured by the two radars, the noise error terms can be determined. Since the same bias error will appear in the density computations from each of the two radar tracks, differencing the densities determines only the noise error terms.

(b) The noise error terms can also be calculated by formulas which directly relate $\sigma_{\dot{z}}$ and $\sigma_{\ddot{z}}$ to N, Δt, σ_z, and the smoothing function. The formulas for polynomial[1] smoothing functions of degrees one and two are given in the following equations:

[1]Polynomials were chosen as the proper class of smoothing functions. This decision was based on previous work showing the polynomial yielding less noise error than other functions.

Noise Error Equations

Velocity:

Linear fit $$\sigma^2_{\dot{x}_1} = \frac{12}{N(N^2 - 1)} \frac{\sigma^2_x}{\Delta t^2}$$

Cubic fit $$\sigma^2_{\dot{x}_3} = \left[\frac{12}{N(N^2 - 1)} + \frac{7(3N^2 - 7)^2(N - 4)!}{(N + 3)!}\right]\frac{\sigma^2_x}{\Delta t^2}$$

Quadratic fit Same as linear fit $\sigma^2_{\dot{x}_2} = \sigma^2_{\dot{x}_1}$

Acceleration:

Linear-linear fit $$\sigma^2_{\ddot{x}_{11}} = \frac{12}{M(M^2 - 1)} \frac{\sigma^2_{\dot{x}_1}}{\Delta t_1^2}$$

Cubic-linear fit $$\sigma^2_{\ddot{x}_{31}} = \frac{12}{M(M^2 - 1)} \frac{\sigma^2_{\dot{x}_3}}{\Delta t_1^2}$$

Cubic-cubic fit $$\sigma^2_{\ddot{x}_{33}} = \left[\frac{12}{M(M^2 - 1)} + \frac{7(3M^2 - 7)^2(M - 4)!}{(M + 3)!}\right]\frac{\sigma^2_{\dot{x}_3}}{\Delta t_1^2}$$

Linear-cubic fit $$\sigma^2_{\ddot{x}_{13}} = \left[\frac{12}{M(M^2 - 1)} + \frac{7(3M^2 - 7)^2(M - 4)!}{(M + 3)!}\right]\frac{\sigma^2_{\dot{x}_1}}{\Delta t_1^2}$$

Quadratic (second derivative) $$\sigma^2_{\ddot{x}_2} = \left[\frac{720}{N^5 - 5N^3 + 4N}\right]\frac{\sigma^2_x}{\Delta t^4}$$

(6)

(Linear polynomial smoothing is defined as fitting a linear polynomial over N data points and assigning the slope of the fit to be the velocity at the midpoint $\frac{N+1}{2}$ of the interval. Linear-linear smoothing to obtain acceleration is described as fitting N position points to a polynomial to obtain velocities and obtain acceleration from velocities in a like manner. A cubic-linear fit is described as fitting N position points to a cubic polynomial taking the slope at the midpoint as the velocity and fitting M of these velocities by a linear polynomial to obtain acceleration; similarly, for cubic-cubic and linear-cubic

smoothing techniques. Quadratic smoothing is defined as fitting a second-degree polynominal to position points and evaluating the first and second derivatives of the polynomial, at the midpoint, as the velocity and acceleration, respectively.) The validity of these formulas has been established by comparisons to RMS errors obtained by method (a).

BIAS ERROR TERMS

The bias errors in velocity and acceleration ($\Delta\dot{z},\Delta\ddot{z}$) depend upon

The type of smoothing technique used
The number of data points (N) used in the smoothing process
The time spacing between consecutive data points (Δt)
The true position field, which itself is a function of the balloon apogee

ESTIMATION OF BIAS ERRORS

For a given apogee, bias errors can be determined by following the flow chart of figure 4. Given a drag table and balloon apogee, by assuming the sphere fell in the 1962 Standard Atmosphere, the equations of motion can be integrated to obtain the theoretical path of the sphere. The vertical position z, velocity $\dot{z}$, and acceleration $\ddot{z}$ are determined by the theoretical trajectory. One now treats the z position as a function of time as though it were the radar coordinates and applies the smoothing routine using N data points and the degree polynomial P. The smoothed z, $\dot{z}$, and $\ddot{z}$ coordinates differ from the theoretical z, $\dot{z}$, and $\ddot{z}$ coordinates only because of the bias error resulting from the smoothing technique. (No noise has been introduced into the data.) The smoothed coordinates are then substituted into the equations of motion using the same drag table, and density is computed. The only difference between this computed density and the original input density, that is, the 1962 Standard Atmosphere density, is due to the bias error induced by the smoothing function. The percent bias error in density is then plotted as the ratio of the computed density to the standard density.

DETERMINATION OF OPTIMUM SMOOTHING TECHNIQUE

The choice of the optimum polynomial and interval for use in the high-altitude program was derived by using the above techniques. Initially, an escape altitude of 125 km was chosen. For each type double smoothing (linear-linear, cubic-linear, linear-cubic, cubic-cubic) the total error in density, defined as the square root of the sum of the noise and bias errors squared, was computed for all possible combinations of N and M. The

noise error was calculated by method (b) (the formulas as given in equations (6)) using $\Delta t = 1/2$ second and σ_z equals 15 meters. The bias error was computed as described in figure 4. Figures 5, 6, and 7 are plots showing the percent bias error (the deviation of the density ratio from 1) and the 1σ confidence bands of the noise error about the bias. None of the combinations of the degree polynomials and smoothing intervals met the design requirements of 5% density accuracy at 100 km. A compromise was necessary to either reduce the altitude requirements, say to 95 km, maintaining the 5% design accuracy requirements or slackening the accuracy requirements to say 9% while maintaining the 100 km altitude range. The former choice was made. Careful analysis of total error plots for all combinations of degree polynomial and N and M resulted in the choice of the 19-21 linear-cubic combination as optimum.

Total error plots were generated in the same fashion using a quadratic polynomial fit and its first and second derivatives for velocity and acceleration. The best smoothing interval for using a quadratic was determined to be 31 data points (fig. 7). In comparing the optimum quadratic and the optimum linear-cubic smoothing techniques, it is easily seen that the 19-21 linear-cubic produced significantly better results in the altitude region from 70 to 100 km. The probable explanation for this is as follows. By fitting two different functions, one to get velocity and the other to get acceleration, it is possible to partially compensate for, say, a positive bias in density due to a velocity error by using a different degree polynomial or different interval to generate accelerations which will produce a negative density bias. This advantage is not present when using a single function for smoothing.

OPTIMUM FITTING FUNCTIONS TO ACQUIRE DENSITIES

After careful consideration of the results of all the above analysis it was decided that the 19-21 linear-cubic smoothing was the optimum fitting function to acquire densities.

SUMMARY OF DENSITY ERRORS USING OPTIMUM REDUCTION

The total percent error in density resulting from a computation using the high-altitude ROBIN program with optimum smoothing cannot be precisely determined because of the unknown accuracy of the drag table and the occurrence of unknown vertical winds. However, the other contributing terms to density errors have been accurately determined using the optimum smoothing interval. They are less than 1% bias error from 30 to 70 km with a noise error of 3% and a bias error from 3% to 5% from 70 to 95 km with a noise error less than 3%.

WINDS

The equation used for computing wind with the falling sphere method is given as

$$W_X = \dot{x} - \frac{\left(\dot{z} - W_Z\right)\left(\ddot{x} + C_X - g_X - \frac{g_X V_B \rho}{m}\right)}{\ddot{z} + C_Z - g_Z - \frac{g_Z V_B \rho}{m}} \tag{7}$$

The variables in equation (7) which may contribute significantly to wind errors are the horizontal and vertical components of velocity and acceleration.

WIND ERROR EQUATIONS

Having retained only those variables which significantly influence the error in a computed wind, the wind equation simplifies to

$$W_X = \dot{x} - \frac{\ddot{x}\dot{z}}{\ddot{z} - g} \tag{8}$$

The first order of approximation to an error in W_X resulting from the errors in the parameters is given by the following equation:

$$dW_X = d\dot{x} - \frac{\dot{z}}{\ddot{z} - g} d\ddot{x} - \frac{\ddot{x}}{\ddot{z} - g} d\dot{z} + \frac{\ddot{x}\dot{z}}{(\ddot{z} - g)^2} d\ddot{z} \tag{9}$$

If the differential error components are considered as noise error with normal distribution, then by taking the variance of equation (9) the noise error in a wind calculation is given as

$$\sigma^2_{W_X} = \sigma^2_{\dot{x}} + \left[\frac{\dot{z}}{\ddot{z} - g}\right]^2 \sigma^2_{\ddot{x}} + \left[\frac{\ddot{x}}{\ddot{z} - g}\right]^2 \sigma^2_{\dot{z}} + \left[\frac{\ddot{x}\dot{z}}{(\ddot{z} - g)^2}\right]^2 \sigma^2_{\ddot{z}} \tag{10}$$

where $\sigma_{\dot{x}}$, $\sigma_{\ddot{x}}$, $\sigma_{\dot{z}}$, and $\sigma_{\ddot{z}}$ are the noise errors in velocity and acceleration due to the noise in the radar data. To determine the bias of a wind measurement resulting from the bias (oversmoothed) velocity and acceleration measurements, equation (9) is again applied. Considering the component differentials as bias error, the square of the bias wind error is given as

$$\Delta^2 W_X = \left[\Delta\dot{x} - \frac{\dot{z}}{\ddot{z} - g}\Delta\ddot{x} - \frac{\ddot{x}}{\ddot{z} - g}\Delta\dot{z} + \frac{\ddot{x}\dot{z}}{(\ddot{z} - g)^2}\Delta\ddot{z}\right]^2 \tag{11}$$

where the Δx, etc., refers to the bias error in the x velocity component. The total wind error $\left(\sigma_{W_{x_{total}}}\right)$ is defined as the square root of the sum of the noise errror variance plus the bias square error and is given as

$$\sigma^2_{W_{x_{total}}} = \sigma^2_{W_x} + \Delta^2 W_x \tag{12}$$

The problem simply stated is to determine the type smoothing (degree) and smoothing intervals which minimize equation (12). As in the case of the density smoothing the noise error will decrease as the smoothing interval increases, and the bias error increases as the smoothing interval increases so that a minimum does exist for equation (12).

MINIMIZATION OF TOTAL WIND ERROR

The calculation of noise error for the wind computation uses equations (6). However, the calculation of the bias error cannot use figure 4 because, with such a variety of wind profiles in nature, choosing one profile to be representative would not be realistic. Besides it was felt that the use of the following bias equations would be more precise:

Bias Error Equations

Position assumed 4th degree over N data points, i.e.,

$$x = A_0 + A_1 t + A_2 t^2 + A_3 t^3 + A_4 t^4$$

Velocity assumed cubic over M data points, i.e.,

$$\dot{x} = B_0 + B_1 t + B_2 t^2 + B_3 t^3$$

Velocity:

Linear fit $$\Delta\dot{x}_1 = \frac{A_3 \Delta t^2 (3N^2 - 7)}{20}$$

Cubic fit $$\Delta\dot{x}_3 = 0$$

Acceleration:

Linear-linear $$\Delta\ddot{x}_{11} = \ddot{x}_{33} - \ddot{x}_{11}$$

Cubic-linear $$\Delta\ddot{x}_{31} = \frac{B_3 \Delta t_1^2 (3M^2 - 7)}{20}$$

Cubic-cubic $$\Delta\ddot{x}_{33} = 0$$

(13)

To use these equations requires a knowledge of the position field of the balloon. This was accomplished by a separate program which utilizes experimental data to compute the coefficients A_3 and A_5. It is beyond the scope of this paper to describe that program.

DETERMINATION OF OPTIMUM SMOOTHING FUNCTIONS

The optimum double smoothing technique is that combination of degree polynomials (cubic-cubic, cubic-linear, linear-linear) and smoothing intervals (N and M) which gives the minimum total wind error. Plots of the total wind error for each type double smoothing and for N-M values of 51-43, 53-11, and 53-25 are presented in figures 8 to 10. These are merely three illustrations of all the possible combinations for feasible values of N and M. After analyzing plots of the types illustrated by figures 8 to 10, it was determined that the 51-43 cubic-cubic smoothing provides optimum wind reduction.

SUMMARY OF WIND ERRORS USING OPTIMUM REDUCTION

With the type smoothing described above, the total wind error remains less than 10 m/sec to altitudes of nearly 100 km. The amount of detail that can be observed at the very high altitudes is, however, limited because of the large altitude layer used in the smoothing. The frequency response curves presented as figure 11 indicate the detail that can be observed. Plotted in this figure is the ratio of the amplitude of a sinusoidal wave after passing through the smoothing filter to the true amplitude of the original. Each curve gives the ratio as a function of wavelength at a specific altitude. For example, at 90 km altitude the amplitude of a 10 km vertical wave would appear to be only 1/5 the amplitude in the reduced data. A 20 km vertical wave would retain 65 percent of its amplitude in the reduced data. As seen from figure 11, for 70 km, wavelengths less than 10 km are largely destroyed so that only a mean wind profile can be ascertained. Below 70 km, wavelengths of 5 km and less will appear in the reduced data.

OPTIMUM PROGRAM DENSITY RESULTS

A series of three Viper-Dart flights were flown at Eglin Air Force Base, Florida, on February 18, 1968, at 18:00, 19:00, and 20:00 zulu. Each flight was tracked by two FPS-16 radars. The flights are identified as Viper-Dart 11, 12, and 13 and the radars as radar 23 and 27. Figure 12 shows the density ratio (compared with the 1962 Standard Atmosphere) for each track of the three flights. For each of the flights, there is excellent agreement between the two FPS-16 radar tracks. The small differences in densities that are observed are commensurate with the noise errors predicted for the 19-21 linear-cubic

smoothing. There are, however, variations in density as observed from flights 1 hour apart, particularly in the altitude region from 62 to 54 km. The cause of these differences is not known. Possible causes are

(a) An actual time fluctuation in density
(b) Special variation in density between the paths of the three spheres
(c) Inaccuracy in the drag table being experienced at different altitudes for the three flights
(d) A change in the vertical motions of the atmosphere

These discrepancies in density, 1 hour apart, are not due to the inability of the radar to accurately track the spheres. Comparison of densities from the two tracks of the same balloon clearly rules this out. Nor are the density discrepancies thought to be a result of balloon collapse or elongation. All balloon collapse checks indicate the balloon is still spherically inflated to at least a 45 km altitude.

OPTIMUM PROGRAM WIND RESULTS

Figures 13 and 14 are plots of the W_x and W_y components for each of the three flights. Both the W_x and W_y components obtained from both tracks of Viper-Dart 11 show nearly identical agreement. Viper-Dart 12 shows good agreement at altitudes below 85 km but only fair agreement above. Viper-Dart 13 gives good agreement only to 84 km. The cause of this decrease in agreement which is beyond what one should anticipate from the total error plots for 51-43 cubic-cubic smoothing (fig. 8) has been investigated and the following results obtained.

The tracks of radar 23 from both Viper-Dart 12 and Viper-Dart 13 flights show large oscillations which did not appear in the tracks of radar 27 from the same flights. Previous experience with FPS-16 tracking data indicates that the oscillations are probably due to a low servo-bandwidth setting. The fact that radar 27 produces a smooth nonoscillating track indicates the oscillations are not real. Further investigation of the effect of the servo on tracking of passive spheres is in order.

SUMMARY OF RESULTS

Essentially there are three ways of determining the accuracy of the density and wind data: equations (6) and (13) and the model simulation outlined in figure 4. The assumptions made in applying equations (6) and (13) and the model given in figure 4 are not precisely met by the data but are exact enough for their purpose, which was to obtain the optimum smoothing technique. The use of double track flights to obtain errors only gives the noise error of the system. The dual tracking wind data shows that the radars need to

be well tuned in order to acquire winds, and that the tracking problem is more critical to winds than to density. Flights close together in time and space should yield system error information provided the time and space separation is small enough to rule out actual changes. One hour apart for density should be small enough to pick up the system errors. Comparison of the curves in figure 12 indicates that there are system errors in density. These system errors can conceivably come from the tracking radar, but they are larger than the equations predict. The system errors are believed to come probably from other elements of the system, sphere shape, or drag table. To strengthen this conclusion, the wind plots (figs. 13 and 14) have to be examined. The accuracy of the wind data does not depend upon the drag table or sphere shape (the last is almost true) but depends rather heavily upon the tracking radar. Figures 13 and 14 show that the wind repeatability is good, which proves that the tracking is good. Therefore, the conclusion is made that the discrepancy in density is not due to radar tracking but to other elements in the system. The dual tracked data agrees well with the noise errors predicted by equation (5) for density and by equation (10) for winds. There is no other proof given here that the predicted bias errors are correct. This proof could come from simultaneous flights of different type sensors.

TEMPERATURE AND PRESSURE

Since the ROBIN is a density and wind sensor, the program optimized these variables. Temperature and pressure errors fall where they may. The results of these parameters for the Viper-Dart flights 11, 12, and 13 are given in figures 15 and 16 without comment.

APPENDIX

SYMBOLS

Units are not given in the symbol list but any consistent set of units may be used in the equations.

A	cross-sectional area of sphere
AMP	amplitude
A_n, B_n	coefficients in bias error equations, $n = 0,1,2,\ldots$ (see eqs. (13))
C_D	drag coefficient
C_x, C_z	Coriolis acceleration in x- and z-direction, respectively
g	gravitational acceleration
g_x, g_z	gravitational acceleration in x- and z-direction, respectively
K	balloon constant
M	number of data points used in acceleration smoothing process
m	mass of sphere
N	number of data points used in velocity smoothing process
t	time
Δt	time spacing between consecutive position data points
Δt_1	time spacing between consecutive volume data points
V_B	volume of balloon
v	relative velocity of balloon, $\left[\left(\dot{x} - W_x\right)^2 + \left(\dot{y} - W_y\right)^2 + \left(\dot{z} - W_z\right)^2\right]^{1/2}$

W_x, W_y	wind velocity in x- and y-direction, respectively
W_z	vertical wind
x,y,z	position coordinates of radar
$\dot{x}$	balloon velocity in x-direction
$\ddot{x}$	balloon acceleration in x-direction
$\dot{y}$	balloon velocity in y-direction
$\dot{z}$	vertical velocity
$\ddot{z}$	vertical acceleration
$\ddot{z}_{th}, \ddot{z}_{emp}$	theoretical and empirical vertical acceleration, respectively
α	density gradient constant
Δq	bias error of parameter q
ρ	density
ρ_0	initial density
σ_q	variance of parameter q

REFERENCES

1. Engler, Nicholas A.: Development of Methods To Determine Winds, Density, Pressure, and Temperature From the ROBIN Falling Balloon. AFCRL-65-448, U.S. Air Force, May 1965. (Available from DDC as AD 630 200.)

2. Engler, Nicholas A.: Report on High Altitude ROBIN Flights, October 1966. AFCRL-67-0433, U.S. Air Force, May 1967. (Available from DDC as AD 657 810.)

3. Luers, J. K.: Estimation of Errors in Density and Temperature Measured by the High Altitude ROBIN Sphere. Proceedings of the Third National Conference on Aerospace Meteorology, Amer. Meteorol. Soc., 1968, pp. 472-477.

4. Goin, Kennith L.; and Lawrence, W. R.: Subsonic Drag of Spheres at Reynolds Numbers From 200 to 10,000. AIAA J. (Tech. Notes), vol. 6, no. 5, May 1968, pp. 961-962.

5. Heinrich, H. G.; Niccum, R. J.; Haak, E. L.; Jamison, L. R.; and George, R. L.: Modification of the Robin Meteorological Balloon. Vol. II – Drag Evaluations. AFCRL-65-734(II), U.S. Air Force, Sept. 30, 1965. (Available from DDC as AD 629 775.)

6. Peterson, J. W.; Hansen, W. H.; McWatters, K. D.; and Bonfanti, G.: Atmospheric Measurements Over Kwajalein Using Falling Spheres. NASA CR-218, 1965.

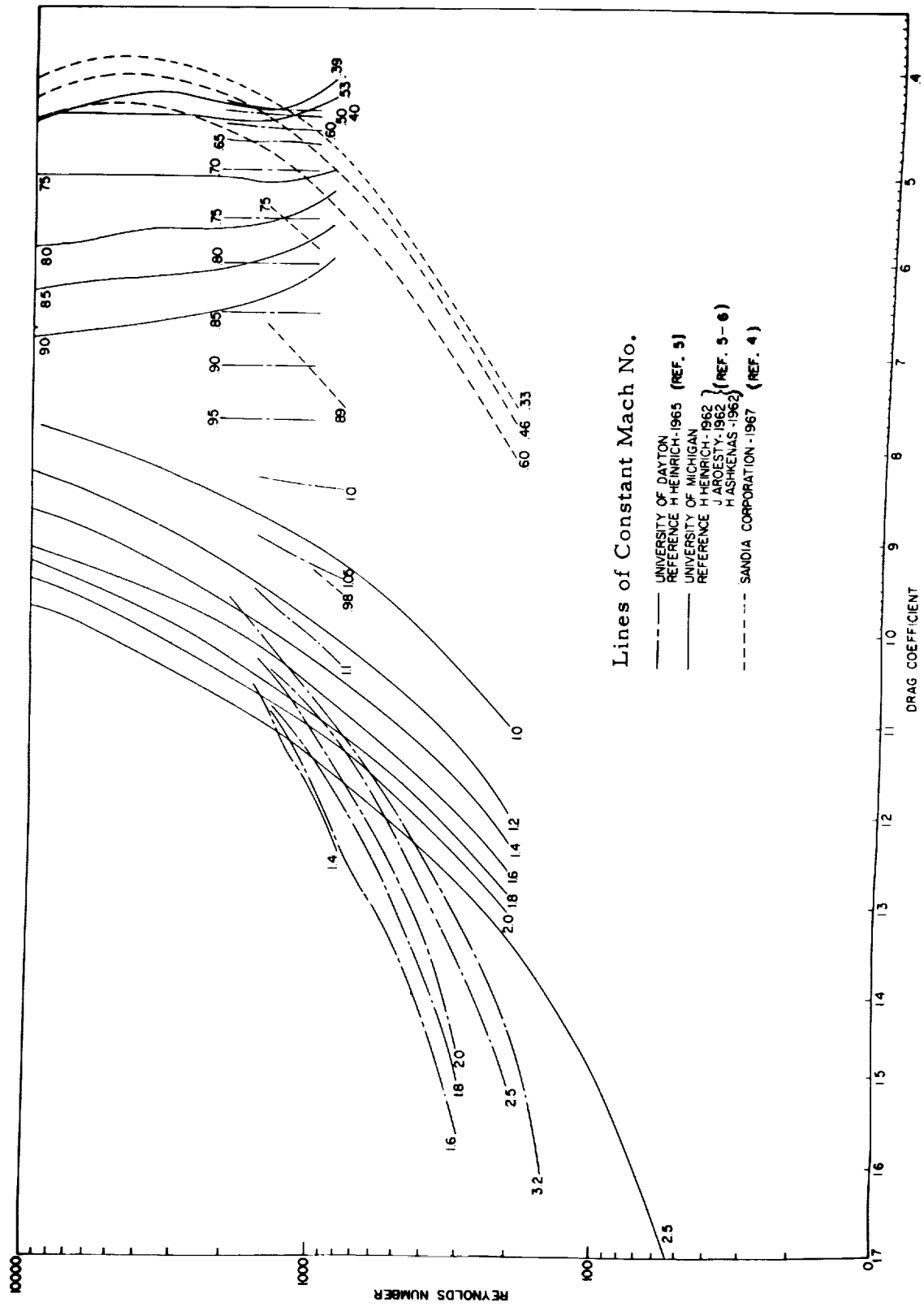

Figure 1.- Drag coefficient as a function of Reynolds number for lines of constant Mach number.

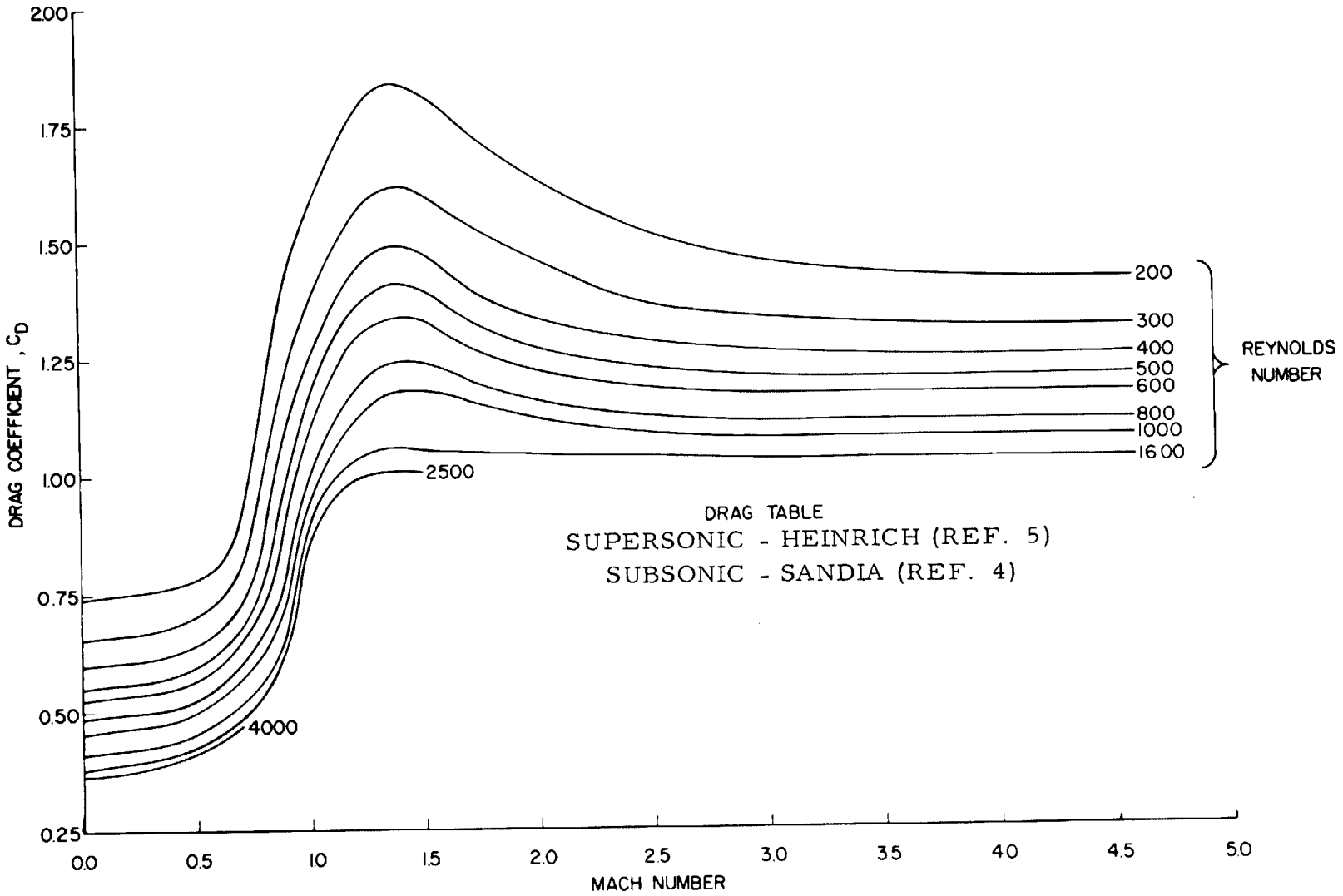

Figure 2.- Drag table derived from Heinrich et al. supersonic data (ref. 5) and Goin and Lawrence subsonic data (ref. 4).

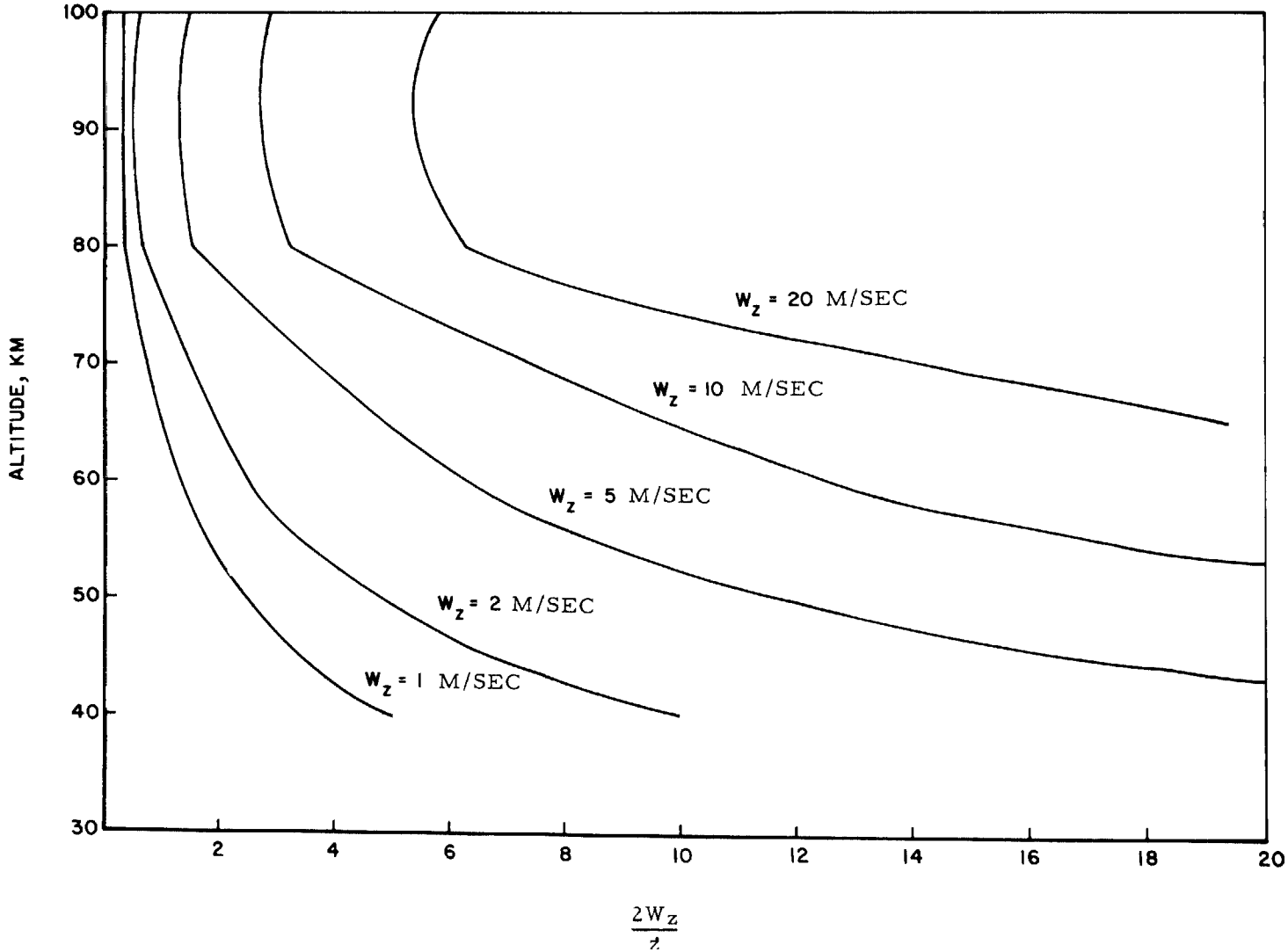

Figure 3.- Density error resulting from vertical winds as a function of altitude. Escape altitude, 125 km.

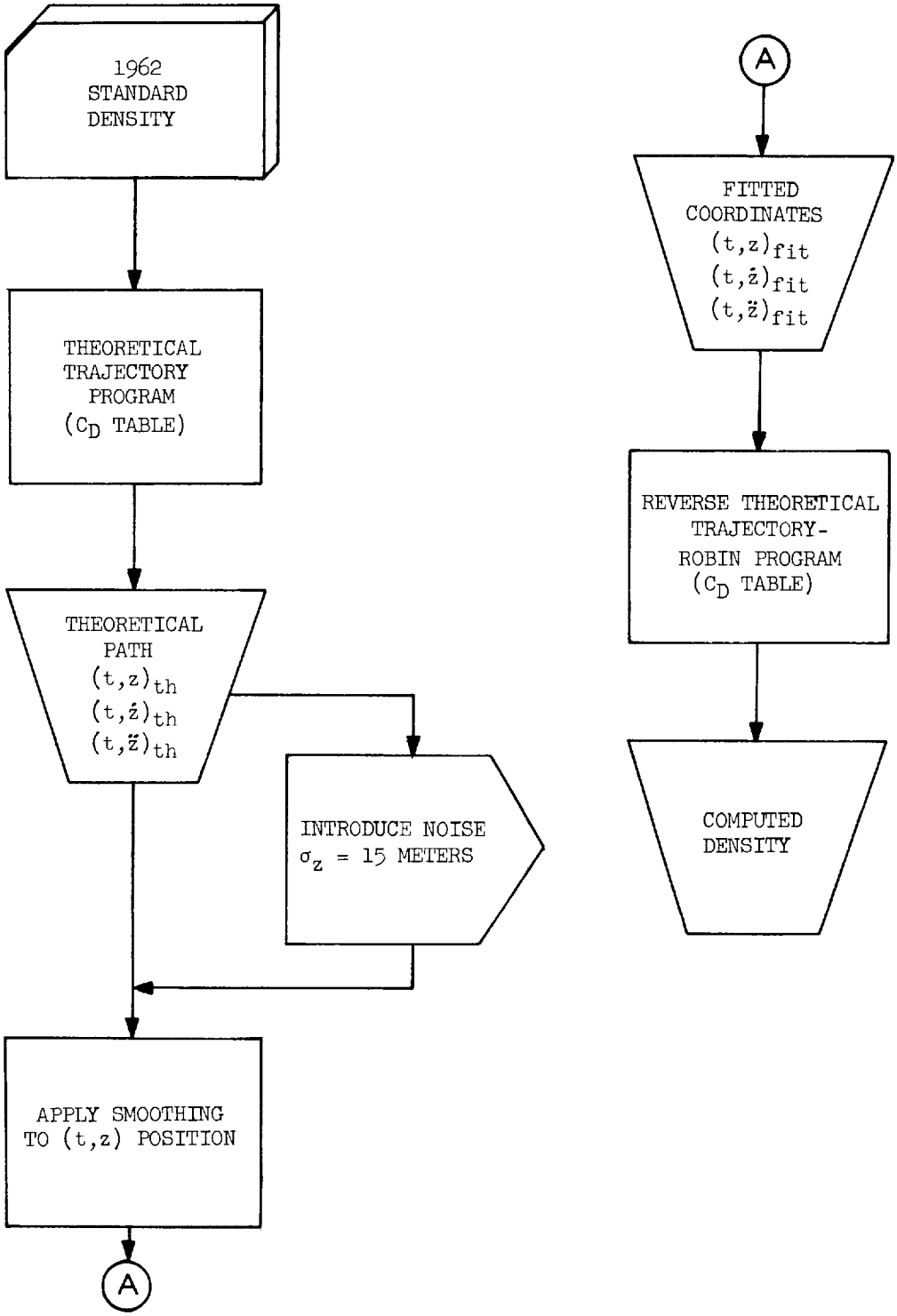

Figure 4.- Flow diagram illustrating procedure used to measure bias error in density.

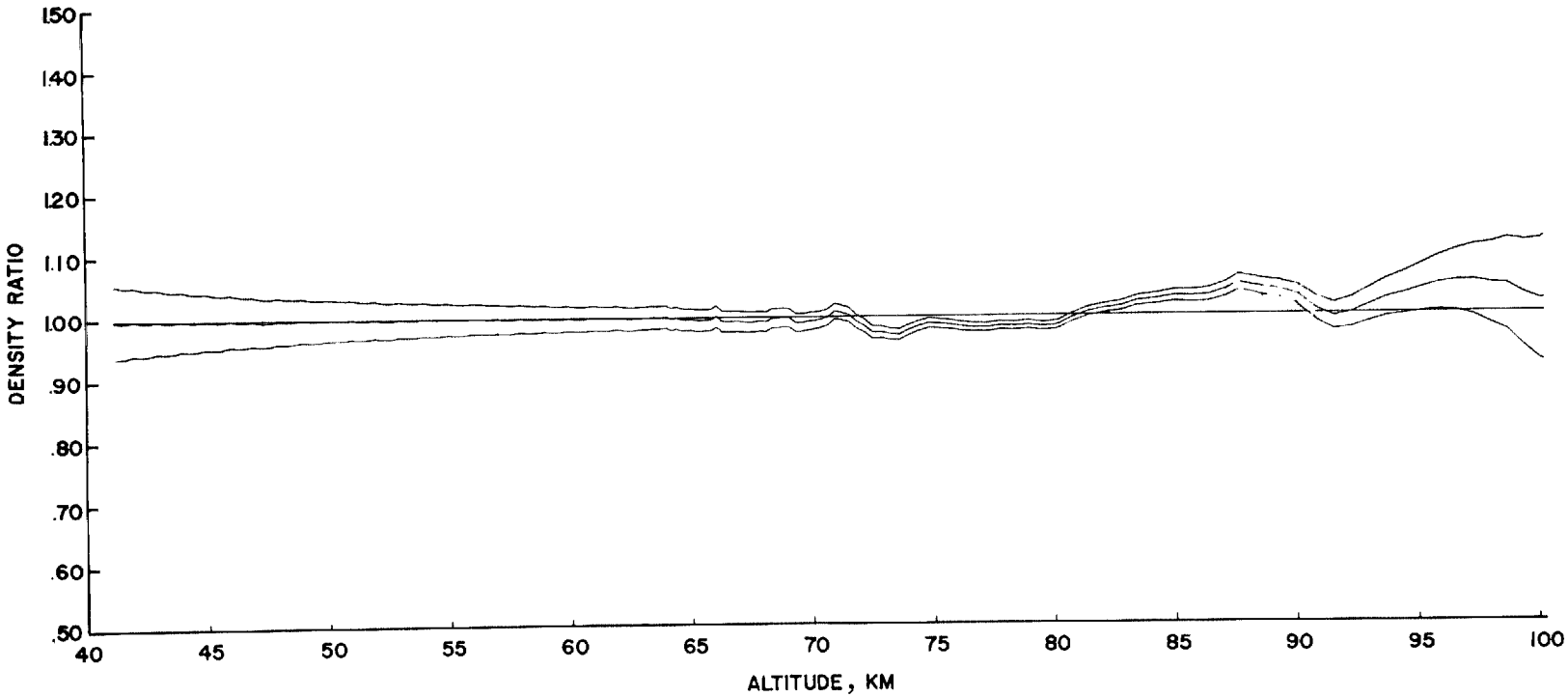

Figure 5.- Ratio of smoothed to standard density (middle curve) using 19-21 linear-cubic smoothing and 1σ noise error about bias.

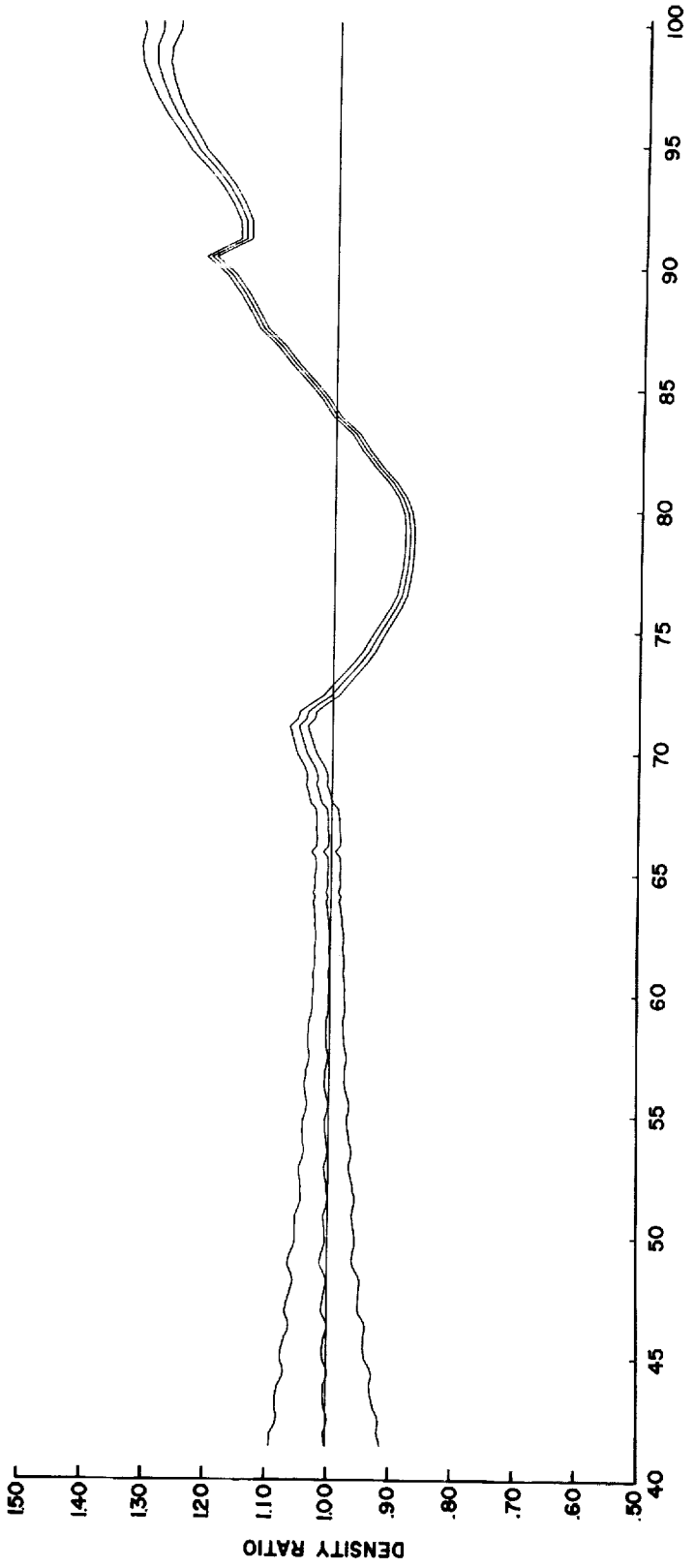

Figure 6.- Ratio of smoothed to standard density (middle curve) using 29-25 cubic-linear smoothing and 1σ noise error about bias.

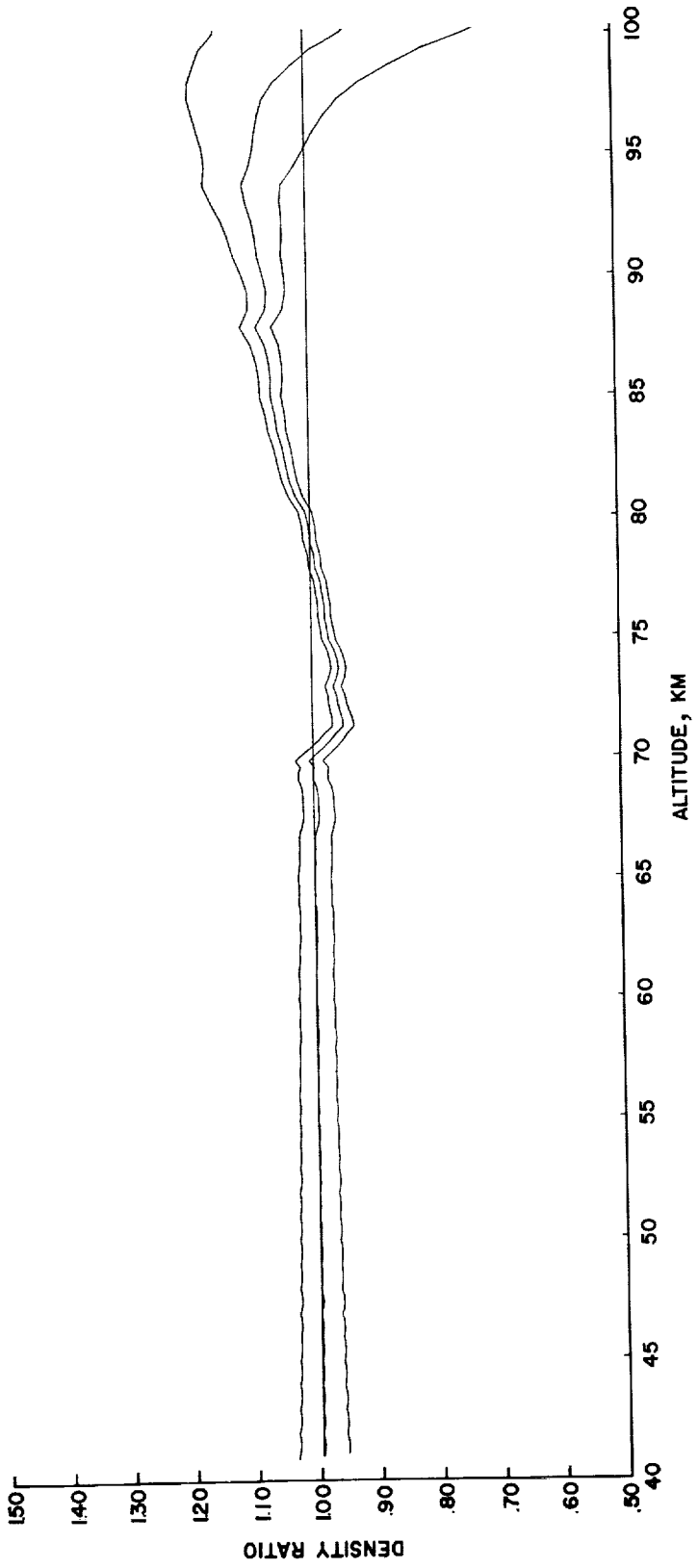

Figure 7.- Ratio of smoothed to standard density (middle curve) using 31 quadratic smoothing and 1σ noise error about bias.

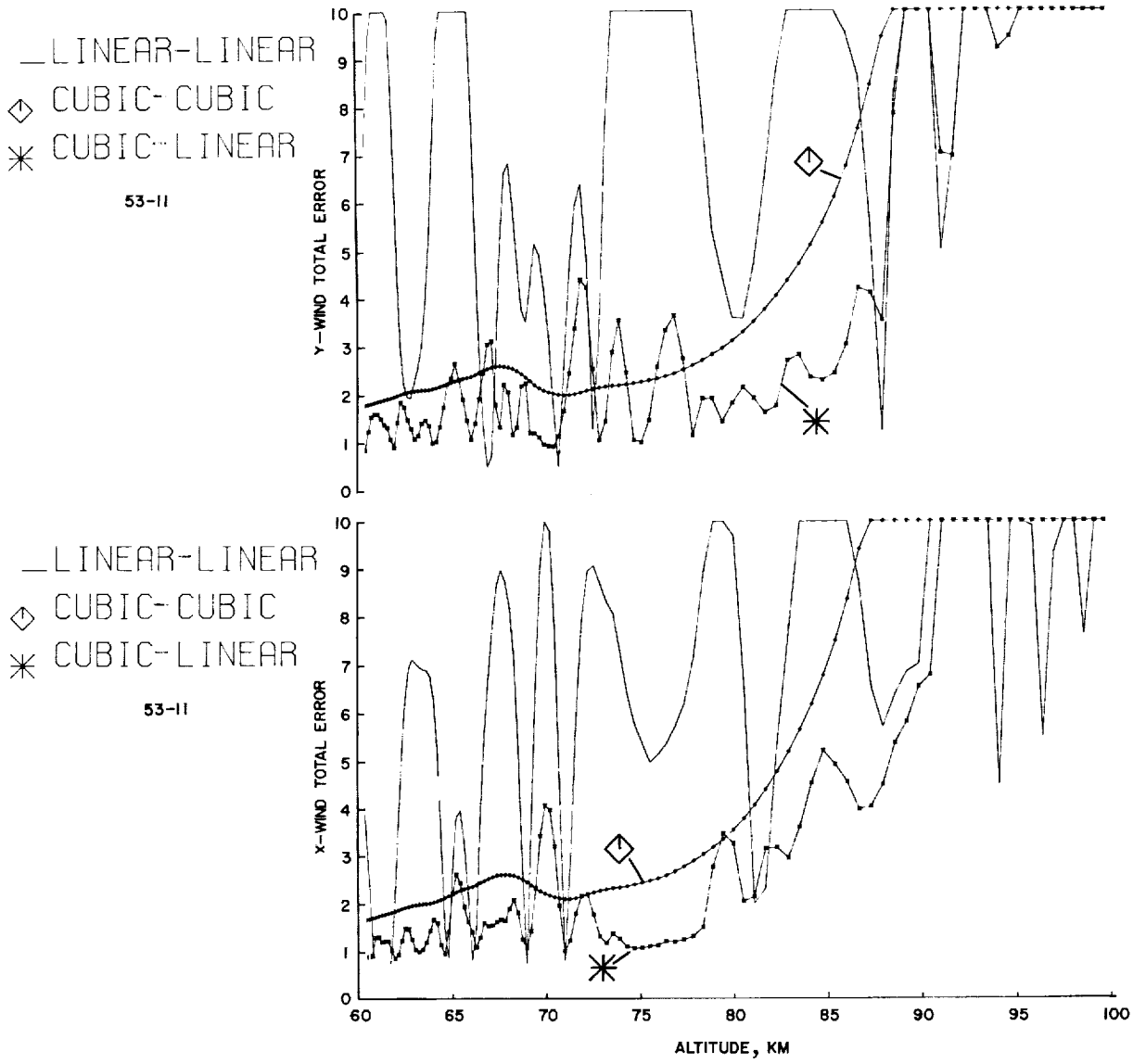

Figure 8.- Total wind error plots for 51-43 cubic-cubic, cubic-linear, and linear-linear smoothing.

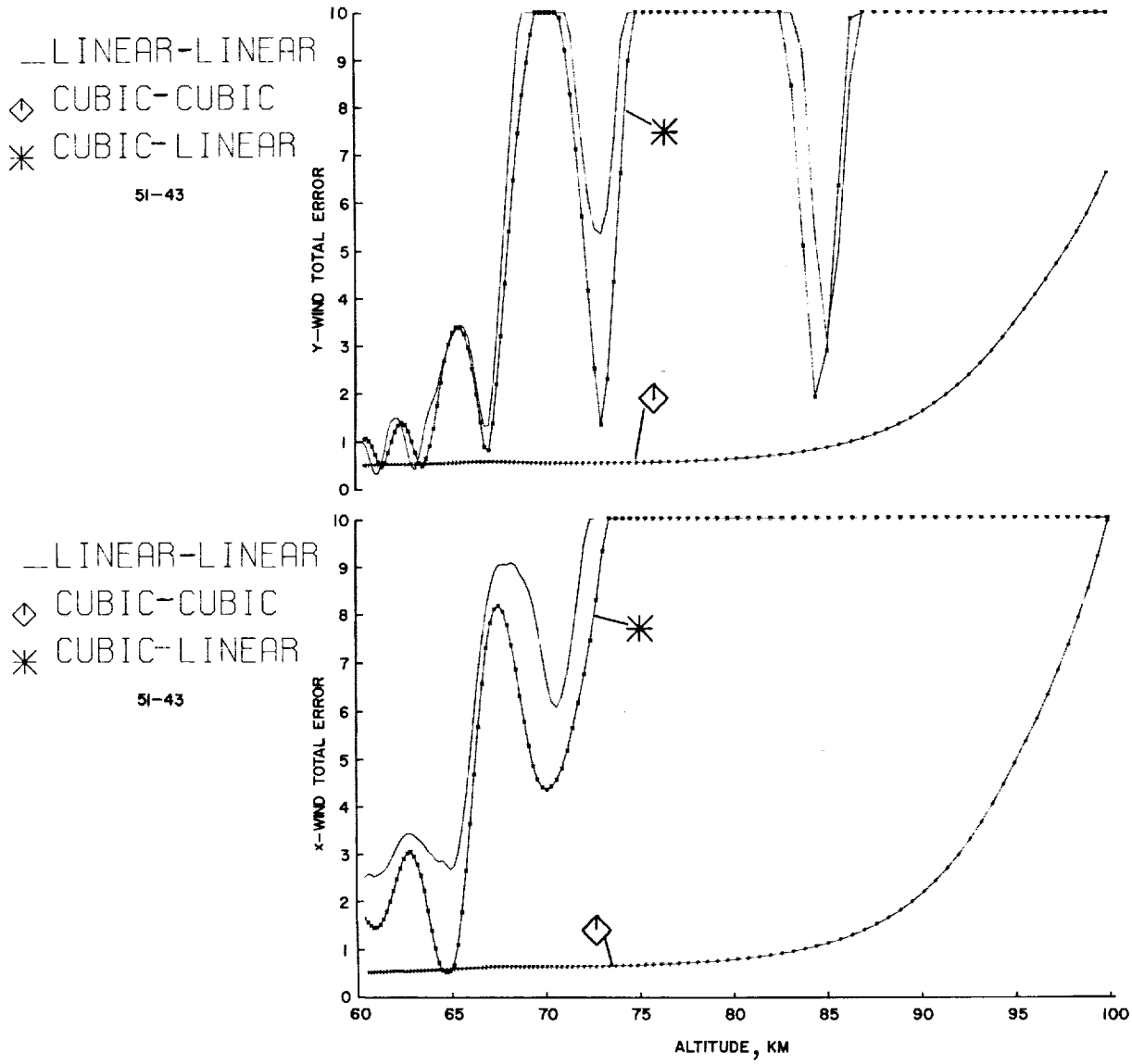

Figure 9.- Total wind error plots for 53-11 cubic-cubic, cubic-linear, and linear-linear smoothing.

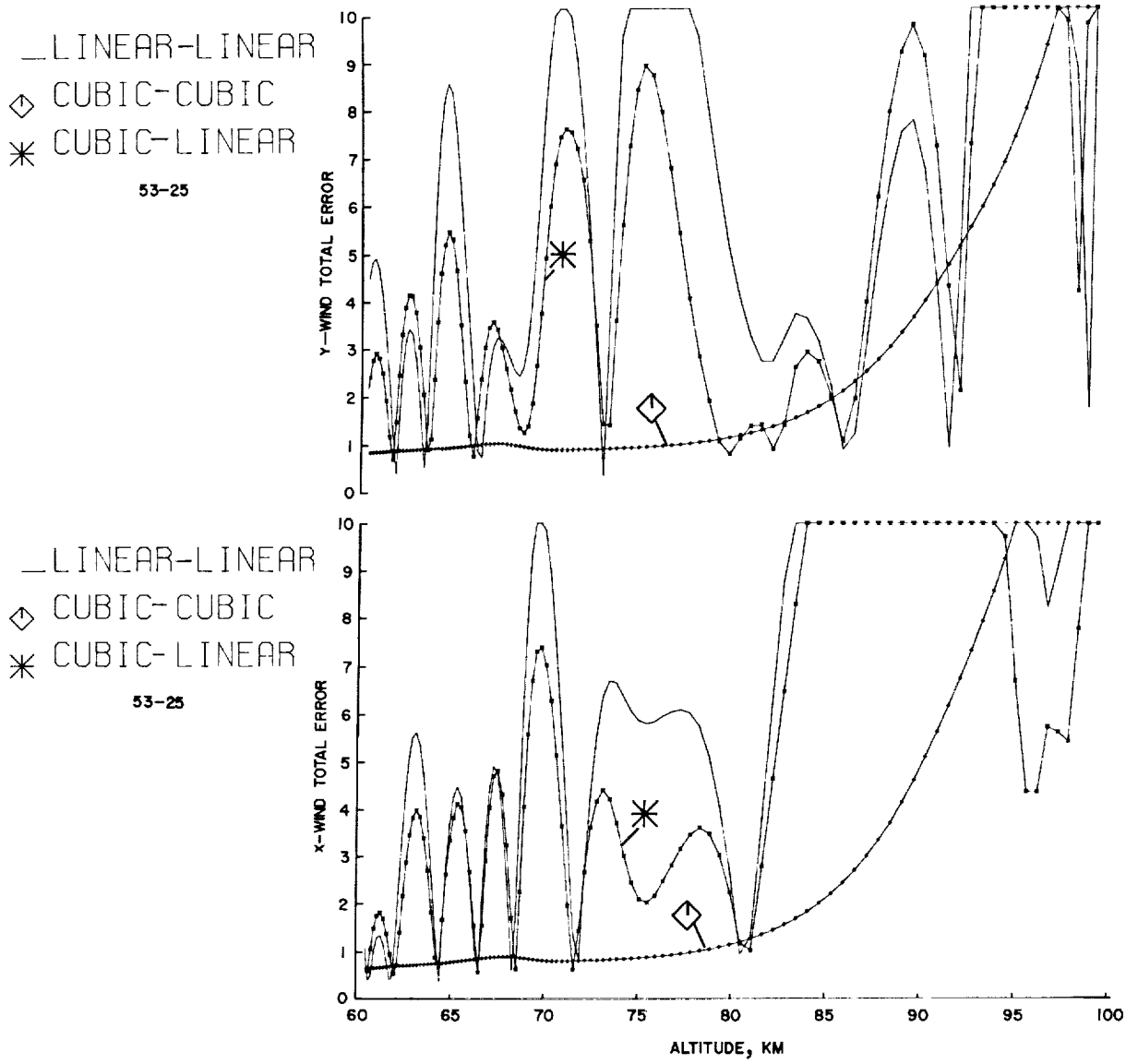

Figure 10.- Total wind error plots for 53-25 cubic-cubic, cubic-linear, and linear-linear smoothing.

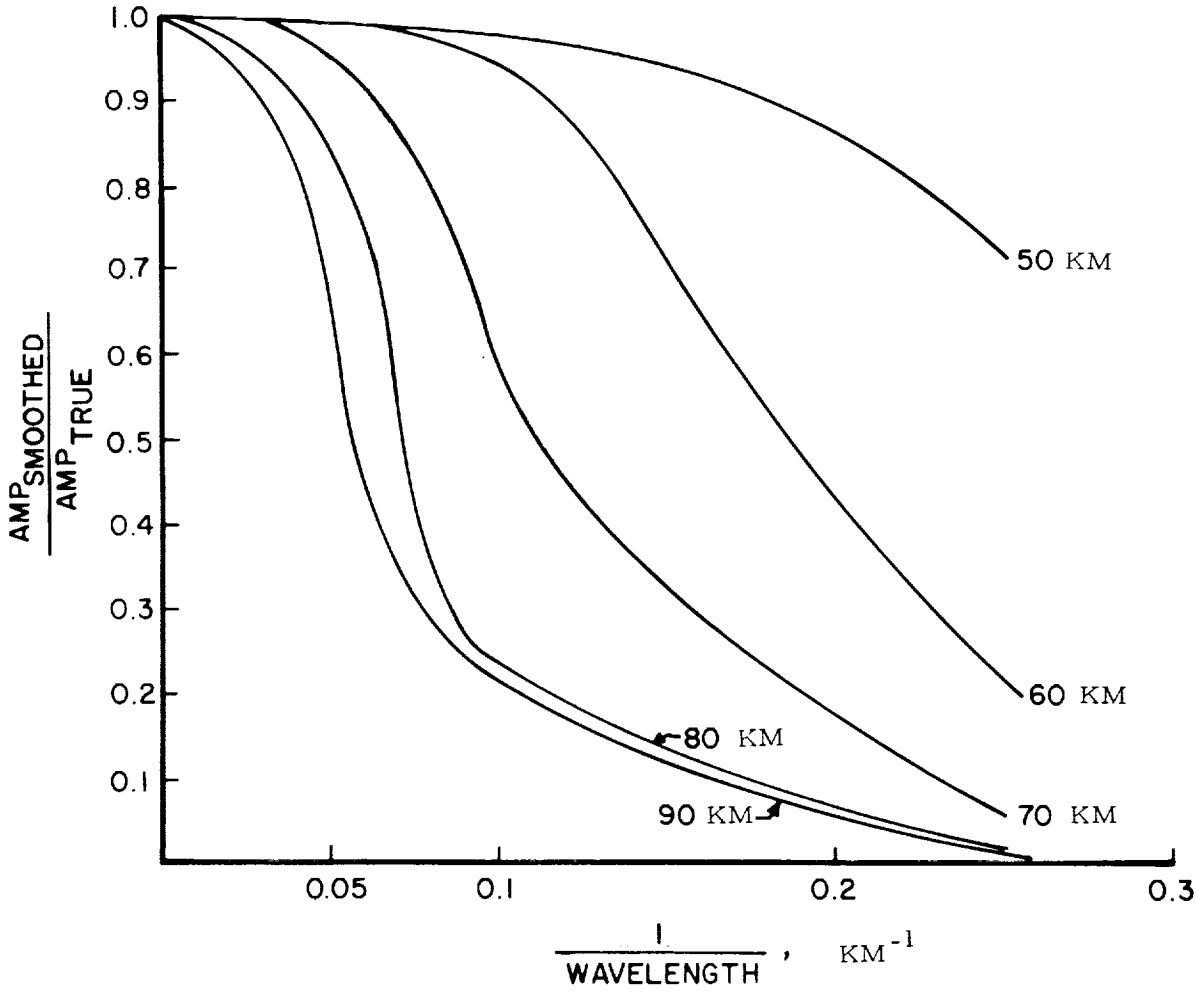

Figure 11.- Ratio of the amplitude of a sinusoidal wave as it would appear in the reduced data to its true amplitude at various altitudes. 51-43 cubic-cubic smoothing; escape altitude, 125 km.

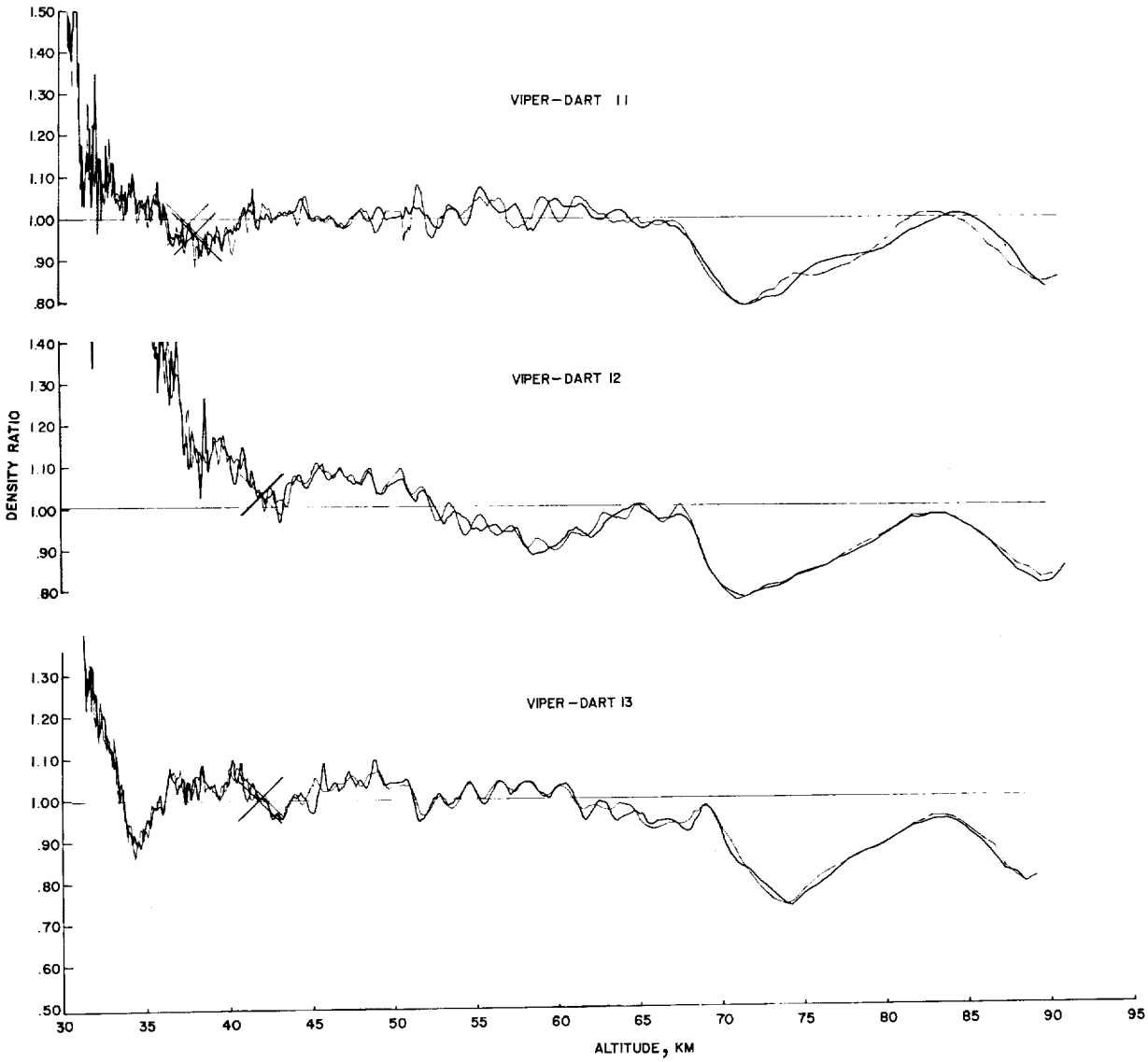

Figure 12.- Ratio of density from Viper-Dart flights 11, 12, and 13 for each radar compared with 1962 Standard Atmosphere density. 19-21 linear-cubic smoothing.

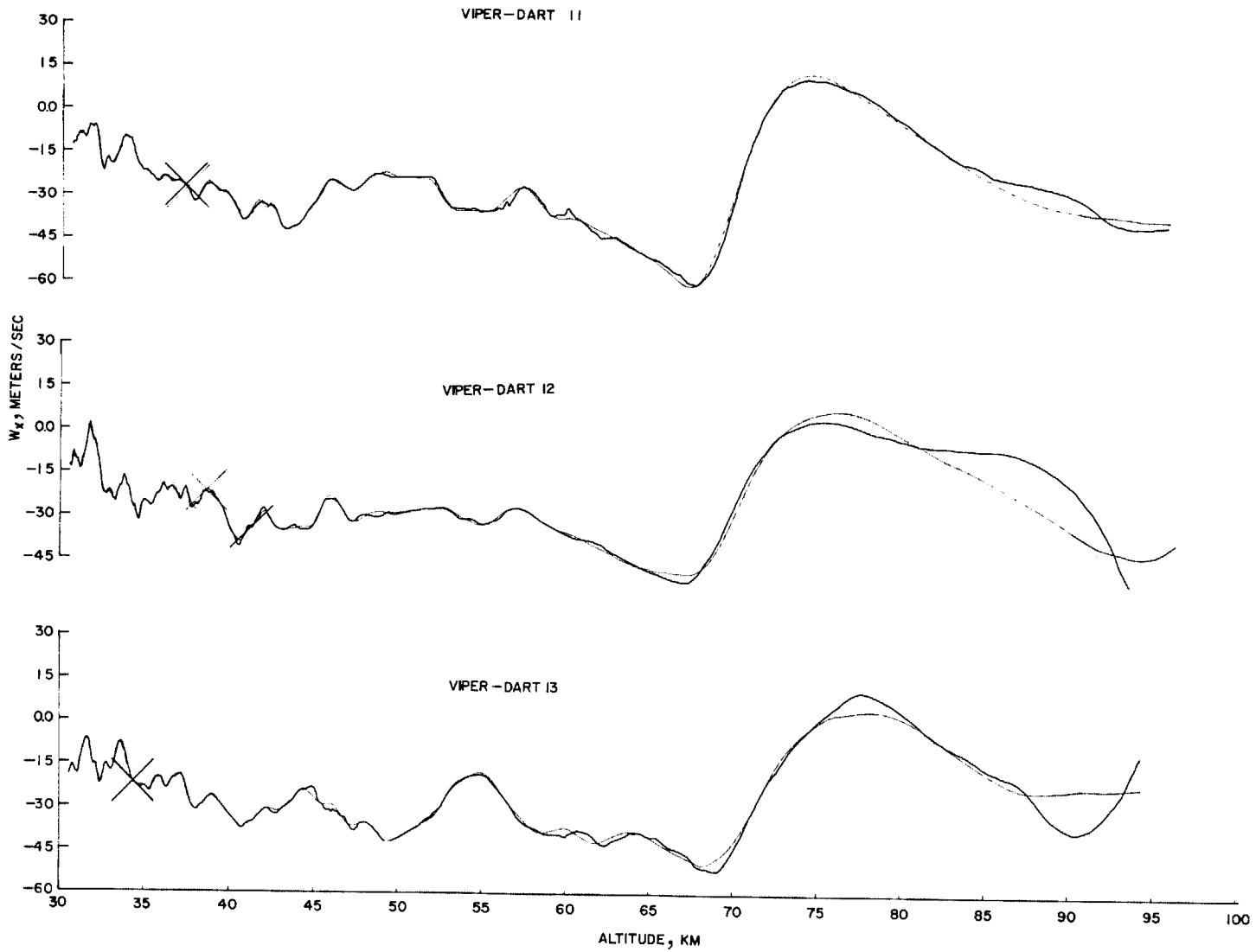

Figure 13.- x-wind component from Viper-Dart flights 11, 12, and 13 for each radar using 51-43 cubic-cubic smoothing.

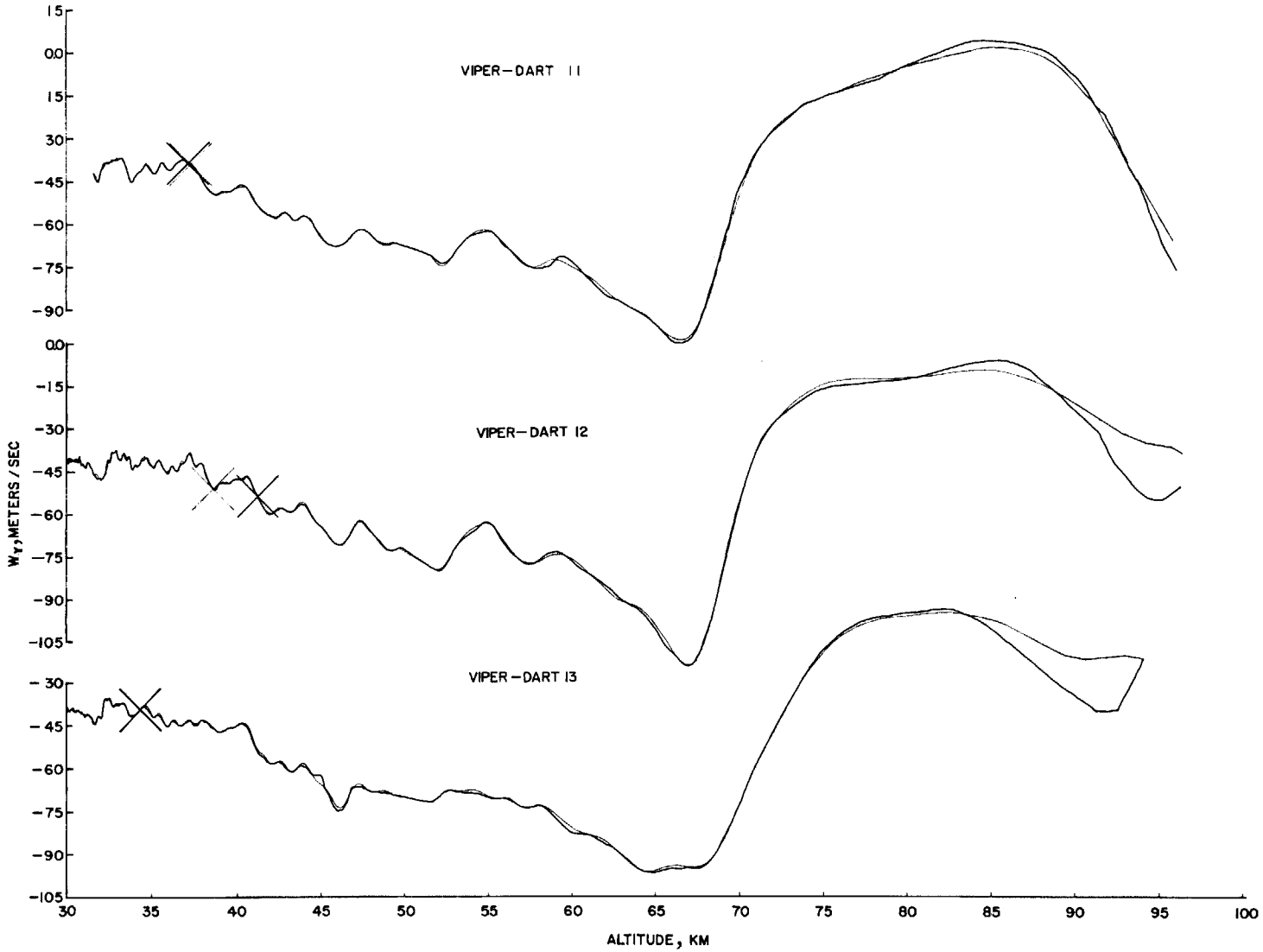

Figure 14.- y-wind component from Viper-Dart flights 11, 12, and 13 for each radar using 51-43 cubic-cubic smoothing.

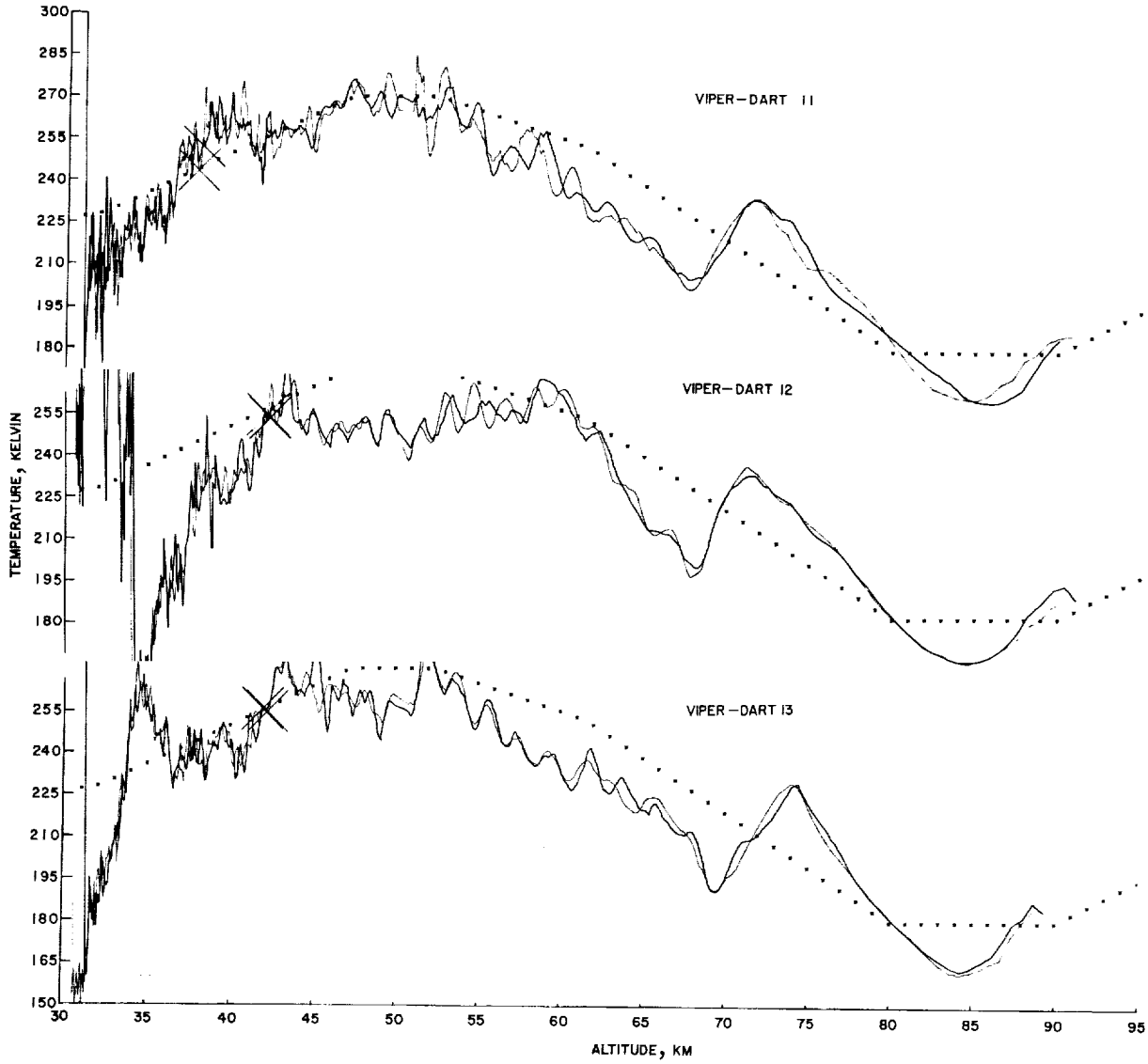

Figure 15.- Temperature from Viper-Dart flights 11, 12, and 13 for each radar compared with 1962 Standard Atmosphere temperature (dotted line) using 19-21 linear-cubic smoothing.

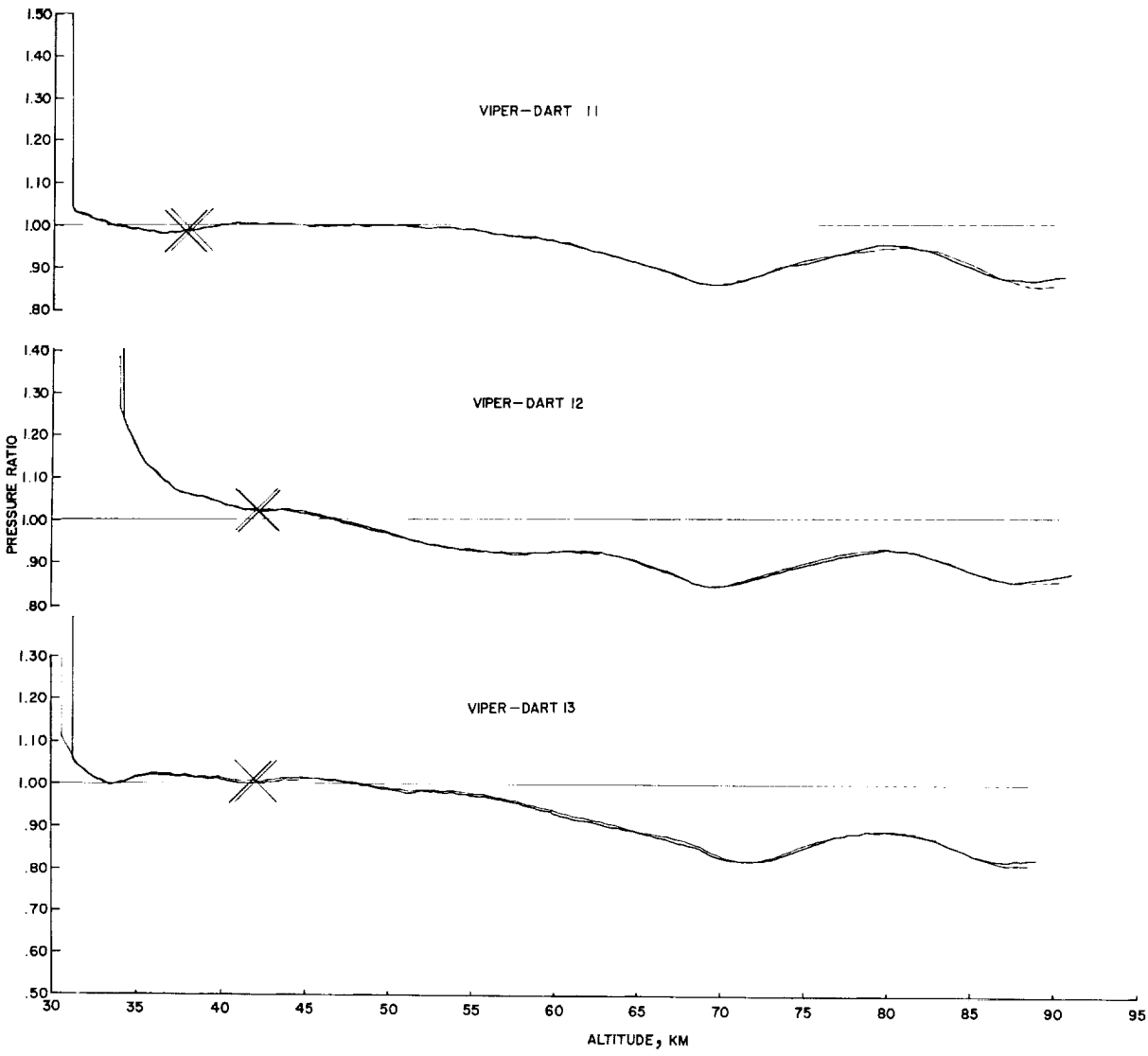

Figure 16.- Ratio of pressure from Viper-Dart flights 11, 12, and 13 for each radar compared with 1962 Standard Atmosphere pressure. 19-21 linear-cubic smoothing.